UNSTEADY LIFT AND DRAG PREDICTIONS USING SIMULATED PSEUDO-TURBULENCE MODELS

T. E. Base

Faculty of Engineering Science,
The University of Western Ontario,
London, Ontario, Canada

and

H. M. Badr*

Mechanical Engineering Department,
King Fahd University of Petroleum & Minerals,
Dhahran, Saudi Arabia

الخلاصـــة :

تمّ في هذا البحث استعمال طريقة عددية لدراسة تأثير الاضطراب فى الانسياب الحر على الطبقة الجدارية اللزجة الثنائية الأبعاد النامية على صفيحة مستوية وتمت دراسة تغير الضغط والقص اللزج وقوى الرفع والمقاومة مع تغير الزمن . واستعمل نموذج حسابي ذو تقنية جديدة نسبياً لمحاكاة (تمثيل) الاضطراب وتزويد الحدود الخارجية لشبكة العناصر المحددة والموضوعة حول الصفيحة بظروف الانسياب المتغيرة . وقد استعملت طريقة الاختلاف لحل معادلات دالة الانسياب وانتقال الدوامية (Helmholtz) بجوار الصفيحة كما تعتمد طريقة التكامل على استخدام العناصر المحددة للتقريب البعدى ونظام كرانك نيكلسون (Crank–Nicolson) المعدل فى اتجاه الزمن . وتمّ رسم التغير الزمنى لمركبات السرعة والدوامية ، وكذلك معاملات قوى الرفع والمقاومة ، كما تم مناقشة النتائج بالتفصيل .

ABSTRACT

In the paper, a numerical method was used to study the effects of free stream pseudo-turbulence on the two-dimensional, viscous layer growing on a flat plate together with the resulting time variations of pressure, viscous shear and lift and drag forces. The approach was to use a relatively new computer simulation technique to generate pseudo-turbulence, which provided the outer boundary conditions to a finite element mesh set around the plate. The variational approach was used to solve the stream function and vorticity transport (Helmholtz) equations near the plate. The method of integration is based on using finite elements for space approximations and a modified Crank–Nicolson scheme for marching in time. The time variation of velocity components, vorticity, and lift and drag coefficients were plotted, and the results were discussed in detail.

*Address for correspondence :
KFUPM Box No. 322
King Fahd University of Petroleum & Minerals
Dhahran 31261
Saudi Arabia

UNSTEADY LIFT AND DRAG PREDICTIONS USING SIMULATED PSEUDO-TURBULENCE MODELS

NOMENCLATURE

c	Length of the plate;
C_D, C_L	Drag and lift coefficients;
D	Drag force;
I	Number of nodal points in the finite element mesh;
I_1, I_2	Variational functionals defined in Equations (12–13);
J	Number of nodes in each element;
k	Total Number of elements in the mesh;
L	Lift force;
M	Total number of vortices in the model;
n	Integer indicating the time level;
N	The element interpolation function;
p	Pressure;
P	Dimensionless pressure defined in Equation 20;
r_c	The vortex viscous core radius;
t	Time;
Δt	Time increment;
u, v	Velocity components in the x, y directions;
u_c	Convection velocity of the vortices ($=u_{ref}$);
x, y	Cartesian coordinates.

Greek symbols

α	A factor denotes an intermediate time level;
Γ	Circulation constant;
ε	A small number;
ξ	The x coordinate of the position of the vortex centre;
ρ	Density;
μ	Dynamic viscosity;
ν	Kinematic viscosity;
η	The y coordinate of the position of the vortex centre;
ψ	The stream function;
ζ	The vorticity;
Ω	The flow domain.

Subscripts

l	Lower surface;
LE	Leading edge;
ref	The reference velocity of the uniform flow with which vortices are convected;
TE	Trailing edge;
u	Upper surface.

Superscripts

(i)	Denotes the element (e_i) in the finite element mesh;
j	Iteration number;
*	Denotes known approximate value.

1. INTRODUCTION

In this study, the unsteady forces on a flat plate are predicted using a new method which involves simulation of the approaching stream using turbulence models and the solution of the viscous flow problem in the vicinity of the plate using a variational finite element method. The turbulence model used is based on the simulation of turbulence by groups of vortices or a series of rotational functions randomly distributed and convected by the approaching stream.

The practical applications of modelling are many, ranging from interaction of aircraft wings with atmospheric turbulence, the response of suspension bridges to unsteady flows and also in the detailed design and aeroelastic stability of jet engine blades.

A comparatively new development in the study of fluid dynamics is the simulation of unsteady fluid flows, such as turbulence, using digital computers: the so called 'computer simulation experiments' or 'synthetic turbulence'. The numerical simulation of two-dimensional turbulence by Lilly [1] and a similar procedure, although independent, by Ahmadi and Goldschmidt [2] have been shown to be important contributions in numerical simulation of pseudo-turbulence. In these two approaches, an incompressible turbulent velocity field was idealized as a random vector field governed in time and two dimensional space by the Navier–Stokes equations. Chorin [3] studied a numerical method for solving the time dependent two-dimensional Navier–Stokes equations at high Reynolds number using a simulation process of vorticity generation and dispersal utilizing computer generated pseudo-random numbers and illustrated the method by solving flow past a circular cylinder. Lesieur and Brissaud [4] also studied a Markovian random coupling model for turbulence.

This field of study is receiving growing attention to the extent that several conferences and lecture series have been held with the main interest being

numerical simulation of turbulent flow, particularly large eddies simulations, to predict the time development of flow fields for engineering applications. The references including the works of Schumann *et al.* [5], Taylor *et al.* [6] and Reynolds [7] represent only a few examples.

In the pseudo-turbulence model developed by Base [8] and reported further by Base and Davies [9], real vortices, randomly distributed representing the turbulent eddy, were convected along in a uniform stream as in Taylor's 'frozen pattern' model of turbulence. This was similar to what has been observed in the turbulent flow far downstream of a grid of bars where the disturbance or eddy can be convected downstream unchanged for a considerable distance and decays very slowly.

Applying the variational approach to solve fluid flow problems has the inherent difficulty of determining the correct functional for the non-linear set of equations. Vooren and Labrujere [10] solved the case of an incompressible, inviscid flow over an aerofoil in a non-uniform field. Bratanow *et al.* [11–13] appear to have developed a more general approach to the unsteady incompressible viscous flow by using the variational approach with applications to flows over oscillating aerofoils. In their solution, however, it was assumed that the velocity field is not sensitive to incremental changes in velocity. The velocity components 'u' and 'v' were approximated by using the Taylor series expansion of velocities in terms of vorticity. It is the opinion of the authors that these approximations and assumptions add some restrictions to the general use of this method. Earlier studies on the application of the finite element method to viscous flow problems include the works of Cheng [14] and Taylor and Hood [15] who studied the time dependent solution of the two-dimensional form of the Navier–Stokes equations.

Numerous research papers have been published recently with emphasis on applications of different finite element methods for solving steady and transient viscous flow problems. A good account of this research can be found in references [16, 17].

2. GOVERNING EQUATIONS

The governing equations of motion for the general transient two-dimensional flow of an incompressible viscous fluid can be written in the form of the Helmholtz vorticity transport equation and the stream function equation as,

$$\frac{\partial \zeta}{\partial t} + \frac{\partial \psi}{\partial y}\frac{\partial \zeta}{\partial x} - \frac{\partial \psi}{\partial x}\frac{\partial \zeta}{\partial y} = \nu \nabla^2 \zeta \qquad (1)$$

$$\zeta = -\nabla^2 \psi \qquad (2)$$

where ψ is the stream function, ζ is the vorticity, t is the time, ν is the kinematic viscosity and $\nabla^2 = \frac{\partial^2}{\partial x^2} + \frac{\partial^2}{\partial y^2}$. The x and y velocity components are related to the stream function by,

$$u = \frac{\partial \psi}{\partial y}, \qquad v = -\frac{\partial \psi}{\partial x}$$

and accordingly the continuity equation is implicitly satisfied.

The relation between the pressure and velocity fields can be obtained from the Navier–Stokes equation and can be written in the form

$$\frac{1}{\rho}\nabla^2 p = 2\left(\frac{\partial u}{\partial x}\frac{\partial v}{\partial y} - \frac{\partial u}{\partial y}\frac{\partial v}{\partial x}\right) \qquad (3)$$

3. UNSTEADY BOUNDARY CONDITIONS

In this section pseudo-turbulent flow models which provided the boundary conditions upstream of the plate and at the two adjacent sides of the finite element mesh are discussed. A new method to determine the transient boundary conditions at the downstream side of the flow field is also introduced.

The approach used to simulate turbulent flow follows the model described in references [8] and [9]. In this model, real vortices representing turbulent eddies were convected along in a uniform stream, similarly as in Taylor's frozen pattern model of turbulence. This is similar to what has been observed in grid turbulence where a disturbance (or eddy) can be convected downstream without a significant change for a considerable distance since the disturbance decay is very slow. Only the continuity equation is satisfied in this model in order to ensure that it is kinematically possible. This has been achieved by a suitable choice of the vortex function. The velocity components u and v and the vorticity ζ at a given point in space vary with time, however, the eddy pattern does not change as it is convected downstream. Figure 1 shows a typical pseudo-turbulent velocity and vorticity variations with time at a particular boundary point upstream of the plate. The method provided a continuous pseudo-turbulent velocity time history at each point on the upstream and side boundaries of the finite element mesh

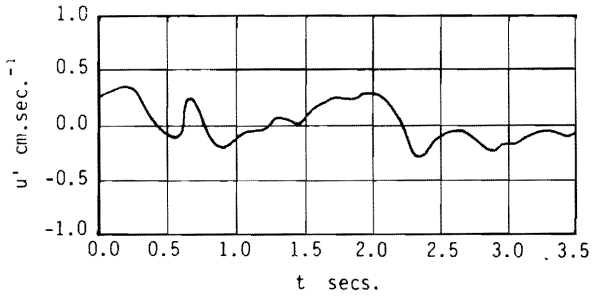

Variation of longitudinal velocity component (u').

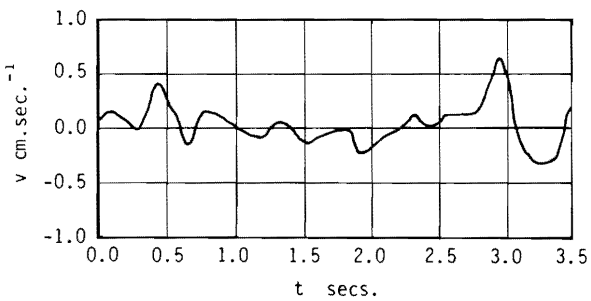

Variation of lateral velocity component (v).

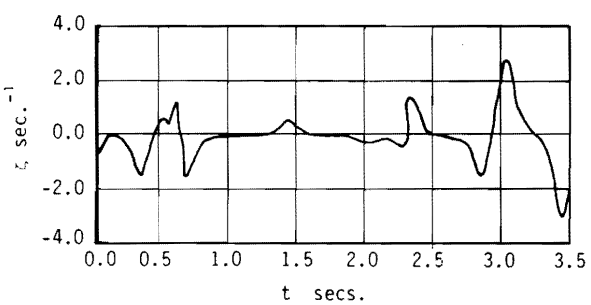

Variation of vorticity (ζ)

Figure 1. Typical Pseudo-Turbulent Variations of Velocity and Vorticity with Time.

shown in Figure 2.

The tacit assumption is that the velocity at any field point (x) is given by the sum of the contributions from the real vortex expressions. The velocity u_i therefore at a boundary point x_i is given by

$$u_i = \sum_{m=1}^{M} (u_i)_m \tag{4}$$

where $(u_i)_m$ is the contribution to the velocity at point x_i due to the mth vortex and M is the total number of vortices representing the model. It can also be shown from Equation (4) that the spacial derivative at any point is also equal to the sum of the derivative contributions from the complete array of vortices so that,

$$\partial u_i/\partial x_i = \sum_{m=1}^{M} (\partial u_i/\partial x_i)_m \tag{5}$$

where $\partial u_i/\partial x_i$ is the spacial derivative at any point x_i. Now, since the condition set for the vortex generating function is mainly to satisfy the continuity equation, so that,

$$(\partial u_i/\partial x_i)_m = 0 \tag{6}$$

then by substituting Equation (6) into Equation (5), one obtains

$$\partial u_i/\partial x_i = 0 \tag{7}$$

The continuity equation is therefore satisfied implicitly throughout the whole vortex model. The velocity field for an individual two-dimensional vortex is obtained by using a stream function expression with the following form,

$$\psi = \frac{\Gamma_1}{\pi} \log_e[r_c^2 + (x - \xi - u_c t)^2 + (y - \eta)^2] \tag{8a}$$

where (x, y) is a field point, (ξ, η) is the initial random position of the vortex in space, Γ_1 is the circulation constant, r_c is the vortex core radius, and u_c is the convection velocity. The corresponding vorticity field for the same vortex is easily obtained by using Equation (2) and can be expressed as

$$\zeta = -\frac{\Gamma_1}{\pi} \frac{2r_c^2}{[r_c^2 + (x - \xi - u_c t)^2 + (y - \eta)^2]^2} \tag{8b}$$

In the numerical solution, the upstream boundary and side boundaries of the flow field are assumed to be completely specified and independent of the conditions inside the flow field. The downstream conditions are obtained by using a new technique which is based on relating the velocities at the downstream side with the velocities at an adjacent section Δx apart at a time delay Δt, where Δx is a small distance and provided that $u > 0$. The relationship between the velocity components at the two adjacent sections can be written as

$$u(x + \Delta x, y, t) = u(x, y, t - \Delta x/u_p) \tag{9}$$

where u_p is the average local convection velocity at the two mesh points (x, y) and $(x+\Delta x, y)$. The boundary conditions at the upper and lower surfaces of the flat plate are the no-slip and impermeability conditions.

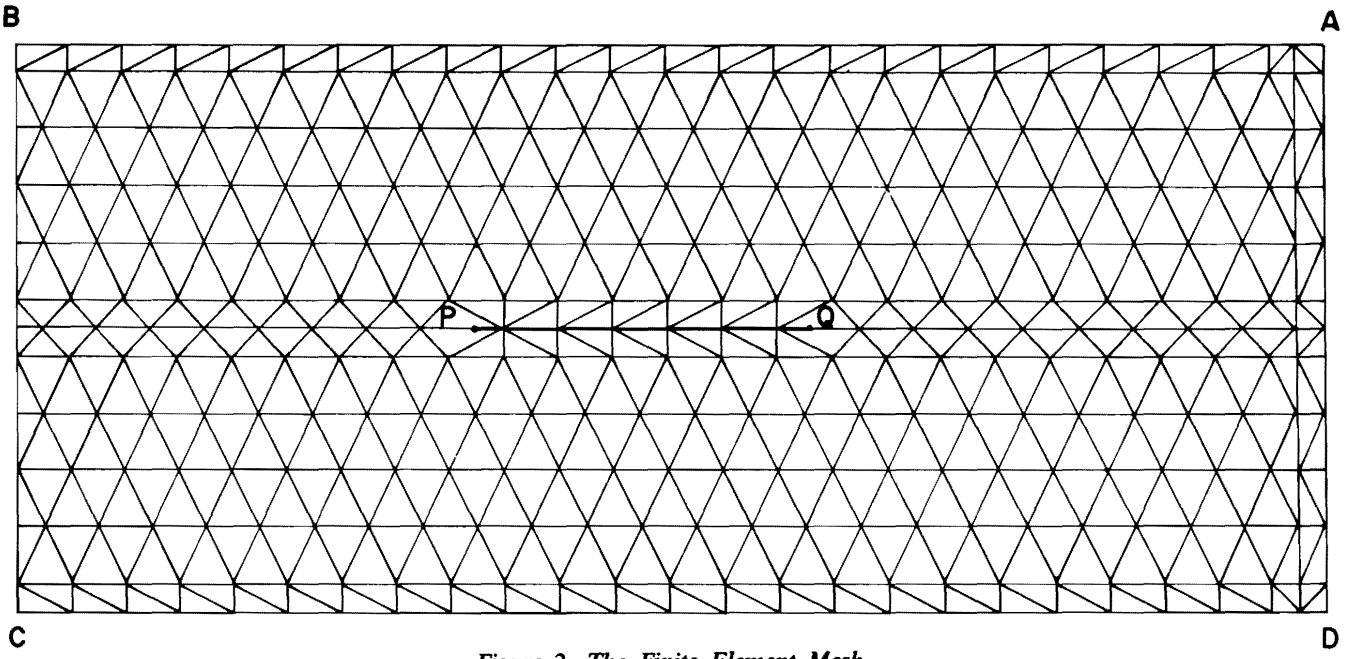

Figure 2. The Finite Element Mesh.

4. THE NUMERICAL SOLUTION

The governing equations (1, 2) subjected to the boundary conditions introduced in Section 3 are integrated using finite elements for space approximations and a modified Crank–Nicolson scheme for marching in time. The method of integration is, in principle, similar to that used by Badr and Base [18]. In this method, the variational functionals of Equations (1, 2) are considered to be exactly the same as that of Poisson's equation with the convective terms in Equation (1) approximated and then corrected using an iterative type solution procedure. In order to give a brief description of the numerical technique, let us assume ψ_n and ζ_n to represent the known stream function and vorticity fields at time $t_n = n\Delta t$ where Δt is the time increment. The problem would be to solve the governing equations (1, 2) to advance the solution of the stream function and vorticity fields to the next time level $t_{n+1} = (n+1)\Delta t$ in order to obtain ψ_{n+1} and ζ_{n+1}. To approximate the nonlinear terms in the vorticity Equation (1) the following linear interpolation formulae are used between the two consecutive time levels t_n and t_{n+1},

$$\left(\frac{\partial\psi}{\partial y}\frac{\partial\zeta}{\partial x}\right)^* = \left\{\alpha\left(\frac{\partial\psi}{\partial y}\right)_{n+1} + (1-\alpha)\left(\frac{\partial\psi}{\partial y}\right)_n\right\}\left\{\alpha\left(\frac{\partial\zeta}{\partial x}\right)_{n+1} + (1-\alpha)\left(\frac{\partial\zeta}{\partial x}\right)_n\right\} \tag{10a}$$

$$\left(\frac{\partial\psi}{\partial x}\frac{\partial\zeta}{\partial y}\right)^* = \left\{\alpha\left(\frac{\partial\psi}{\partial x}\right)_{n+1} + (1-\alpha)\left(\frac{\partial\psi}{\partial x}\right)_n\right\}\left\{\alpha\left(\frac{\partial\zeta}{\partial y}\right)_{n+1} + (1-\alpha)\left(\frac{\partial\zeta}{\partial y}\right)_n\right\} \tag{10b}$$

where α is a constant ranging between 0 and 1 and the superscript * denotes known approximate values. Applying Equation (1) at an intermediate time level $t_{n+\alpha} = (n+\alpha)\Delta t$ and using Equation (10), one obtains

$$\left(\frac{\partial\zeta}{\partial t}\right)_\alpha + \left[\frac{\partial\psi}{\partial y}\frac{\partial\zeta}{\partial x}\right]^* - \left[\frac{\partial\psi}{\partial x}\frac{\partial\zeta}{\partial y}\right]^* = \nu\nabla^2\zeta_\alpha \tag{11}$$

where the subscript α represents the time $t_{n+\alpha}$. Now, considering the term $(\partial\zeta/\partial t)_\alpha$ in Equation (11) as an invariant, the variational functional can be written as

$$I_1(\zeta_\alpha) = \iint_\Omega \left\{\left[\left(\frac{\partial\zeta}{\partial t}\right) + \left(\frac{\partial\psi}{\partial y}\frac{\partial\zeta}{\partial x}\right)^* - \left(\frac{\partial\psi}{\partial x}\frac{\partial\zeta}{\partial y}\right)^*\right]\zeta_\alpha + \frac{\nu}{2}\left[\left(\frac{\partial\zeta_\alpha}{\partial x}\right)^2 + \left(\frac{\partial\zeta_\alpha}{\partial y}\right)^2\right]\right\} dx\, dy \tag{12}$$

The variational functional of Equation (2) at t_{n+1} takes the form,

$$I_2(\psi_{n+1}) = \iint_\Omega \left\{\tfrac{1}{2}\left[\left(\frac{\partial\psi_{n+1}}{\partial x}\right)^2 + \left(\frac{\partial\psi_{n+1}}{\partial y}\right)^2\right] - \psi_{n+1}\zeta_{n+1}\right\} dx\, dy \tag{13}$$

where Ω is the solution domain.

The variations of the stream function ψ and vorticity ζ within each element (e_i) are approximated using linear interpolation functions and can be expressed as,

$$\psi^{(i)} = \sum_{j=1}^{J} N_j(x,y)\psi_j = [N]^{(i)}\{\psi\}^{(i)} \qquad (14a)$$

$$\zeta^{(i)} = \sum_{j=1}^{J} N_j(x,y)\zeta_j = [N]^{(i)}\{\zeta\}^{(i)} \qquad (14b)$$

where J is the number of nodes in each element, $N_j(x,y)$ are the element shape functions, [ ] denotes a row matrix and { } denotes a column matrix. Using Equation (14) in Equations (12) and (13) and writing

$$\left(\frac{\partial\zeta}{\partial t}\right)_\alpha \cong (\zeta_{n+1}-\zeta_n)/\Delta t\,, \qquad \frac{\partial}{\partial x}[N]^{(i)} \text{ as } [N_x]^{(i)} \text{ and}$$

$$\frac{\partial}{\partial y}[N]^{(i)} \text{ as } [N_y]^{(i)},$$

one can write the functionals I_1 and I_2 in terms of the element shape functions as,

$$I_1(\zeta_\alpha) = \sum_{i=1}^{k} \iint_{e_i} \left\{ \left[\frac{1}{\Delta t}[N]^{(i)}(\{\zeta_{n+1}\}-\{\zeta_n\}) + [N_y]^{(i)}\{\psi_\alpha^*\}^{(i)}[N_x]^{(i)}\{\zeta_\alpha^*\}^{(i)} - [N_x]^{(i)}\{\psi_\alpha^*\}^{(i)}.[N_y]^{(i)}\{\zeta_\alpha^*\}^{(i)} \right][N]^{(i)}\{\zeta_\alpha\}^{(i)} + \frac{\nu}{2}\left[\left([N_x]^{(i)}\{\zeta_\alpha\}^{(i)}\right)^2 + \left([N_y]^{(i)}\{\zeta_\alpha\}^{(i)}\right)^2 \right] \right\} dx\, dy \qquad (15)$$

and

$$I_2(\psi_{n+1}) = \sum_{i=1}^{k} \iint_{e_i} \left\{ \tfrac{1}{2}\left[\left([N_x]^{(i)}\{\psi_{n+1}\}^{(i)}\right)^2 + \left([N_y]^{(i)}\{\psi_{n+1}\}^{(i)}\right)^2 \right] - [N]^{(i)}\{\psi_{n+1}\}^{(i)}.[N]^{(i)}\{\zeta_{n+1}\}^{(i)} \right\} dx\, dy \qquad (16)$$

where k is the number of elements in the finite element mesh.

The extremization of the functionals I_1 and I_2 with respect to each of the nodal values of ζ_α and ψ_{n+1} is necessary to satisfy the governing equations and by approximating ζ_α using the following linear interpolation formula,

$$\zeta_\alpha = \alpha\,\zeta_{n+1} + (1-\alpha)\,\zeta_n\,,$$

the resulting set of linear algebraic equations can be written in the form of a simple matrix problem for each of $\{\zeta_{n+1}\}$ and $\{\psi_{n+1}\}$.

The solution started at $t=0$ with the stream function and vorticity fields assumed to be exactly the same as the steady conditions that would prevail when no disturbances are present in the approaching stream. The solution of this problem is exactly the same as given in reference [18]. The sequence of the solution to advance the ψ and ζ fields through one time step Δt is to assume, as a first approximation, that ψ_{n+1} and ζ_{n+1} to be the same as ψ_n and ζ_n respectively ($n=0$ at the start of the solution). Equation (10) is then used to approximate the nonlinear terms in Equation (15) and the matrix problem resulting from the extremization process is then solved to obtain a better approximation for ζ_{n+1}. The new values of ψ_{n+1} are then obtained by solving the set of algebraic equations resulting from the extremization of I_2. The new values of ψ_{n+1} and ζ_{n+1} are then used in Equation (10) to obtain a better approximation for the non-linear terms. This iterative process continues until the following convergence criteria are satisfied

$$\sum_{i=1}^{I}\left|\left(\frac{\zeta_{n+1}^{j+1}-\zeta_{n+1}^{j}}{\zeta_{n+1}^{j+1}}\right)_i\right| < \varepsilon \quad \text{and} \quad \sum_{i=1}^{I}\left|\left(\frac{\psi_{n+1}^{j+1}-\psi_{n+1}^{j}}{\psi_{n+1}^{j+1}}\right)_i\right| < \varepsilon \qquad (17)$$

where i is the nodal point number, I is the total number of nodal points in the finite element mesh, ε is small number ($\simeq 10^{-4}$), and the superscript j denotes the iteration number. After convergence is achieved the solution continues to the following time level.

The pressure gradient on each side of the flat plate positioned at $y=0$ can be obtained from the velocity field by applying the x-component of the Navier–Stokes equations at the plate and using the no-slip and impermeability conditions which results in,

$$\left(\frac{\partial p}{\partial x}\right)_{y=0} = \mu\left(\frac{\partial^2 u}{\partial y^2}\right)_{y=0} = \mu\left(\frac{\partial\zeta}{\partial y}\right)_{y=0} \qquad (18)$$

Now, define the dimensionless pressure P such that,

$$P = \frac{p_{LE}-p}{\frac{1}{2}\rho\, u_{ref}^2} \qquad (19)$$

where p_{LE} is the pressure at the leading edge, p is the local pressure at any section x on the plate (measured from the leading edge downstream), and

u_{ref} is the reference velocity with which vortices are convected. Using Equations (18) and (19), one can easily deduce,

$$P(x) = \frac{-2\nu}{u_{ref}^2} \int_0^x \left(\frac{\partial \zeta}{\partial y}\right)_{y=0} dx \qquad (20)$$

A simple integration scheme was used to obtain the pressure distribution on the upper and lower surfaces of the plate from the known vorticity field. Further details of the numerical method can be seen in reference [18].

The accuracy of the numerical method was verified by considering two problems. The first one was that of the viscous decay of a single concentrated vortex for which an exact analytical solution is known. The second problem was the steady two-dimensional viscous developing flow in the entrance region of a straight channel with flat parallel walls. An analytical solution for this problem based on series expansion method was obtained by Schlichting [19]. The comparison between the time variation of the vorticity distribution in the first problem and the velocity profiles in the second one resulted in very good agreements with the analytical solutions. More details can be seen in reference [18].

5. THE RESPONSE OF A FINITE THIN FLAT PLATE TO AN APPROACHING PSEUDO-TURBULENT FLOW

The problem considered was that of a thin flat plate set at zero incidence to an initially uniform flow with velocity u_{ref}. A finite element mesh was set around the plate as shown in Figure 2. Upstream and away from the influence of the plate, finite groups of randomly positioned vortices representing the oncoming eddy structure were set up and allowed to move with the free stream towards the plate. To illustrate the flow domain and the method of analysis, the diagram shown in Figure 3 has five boxes with the center box subdivided into additional three boxes. The flat plate *PQ* is positioned midway between the two sides *AB* and *CD* of the box *ABCD* as shown.

With the increase of time, the vortices assembled randomly in box number 1 are convected toward the plate and replaced with another set until the first four boxes are filled with vortices. With further increase in time and with no further increase in the number of vortices being added to the model, the program is so scaled that within a given time period the vortices move approximately one box length downstream. Approximately one quarter of the total number of vortices furthest downstream, that have little influence at the outer boundary points of the finite element mesh stencil (*ABCD*), were now removed and replaced by the same number of similar vortices with new random positions and new signs upstream of the plate where again the vortices have little influence on the conditions at the mesh boundaries.

The vortex model then continued and the process repeated again so that a continuous pseudo-turbulent flow field is simulated. By this means, therefore, the vortex model provided the unsteady velocity field at the outer grid points along the boundaries *AB*, *BC*, and *CD* of the finite element mesh. Accordingly, the effect of the pseudo-turbulence entered the flow domain in the form of time-dependent boundary conditions. The unsteady flow was convected and diffused within the stencil and finally modified the flow over the plate.

The shear stresses on the upper and lower surfaces of the flat plate were integrated to determine the time variation of the skin friction drag. The integration of pressure obtained from Equation (19) and (20) on the upper and lower sides of the plate

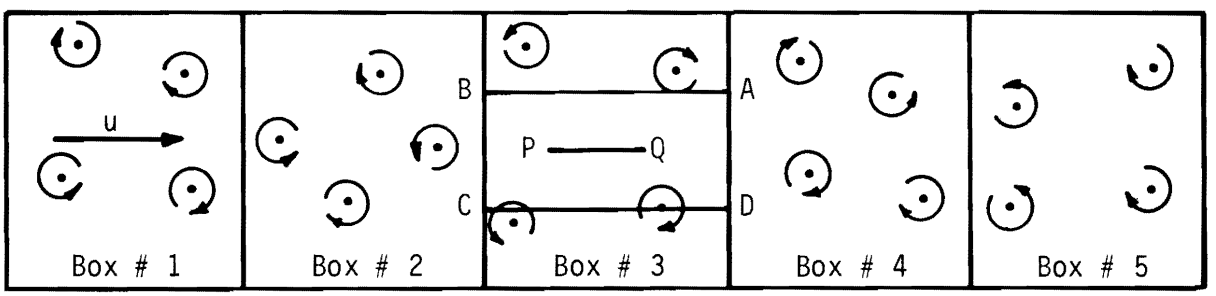

Figure 3. Schematic Diagram of the Flow Field Divided into Five Boxes with the Flat Plate PQ *Placed Midway Between the two Sides* AB *and* CD *of the Solution Domain* ABCD.

provided the time variation of the overall lift. The lift and drag coefficients are defined as,

$$C_L = \frac{L}{\frac{1}{2}\rho u_{ref}^2 A}, \qquad C_D = \frac{D}{\frac{1}{2}\rho u_{ref}^2 A} \tag{21}$$

where L is the lift force, D is the drag force and A is the area of the plate. The relationship between the drag coefficient and the vorticity field can be written as,

$$C_D = \frac{\nu}{c\, u_{ref}^2} \int_0^c (\zeta_l - \zeta_u)\, dx \tag{22}$$

where c is the length of the plate and the subscripts l and u denote the lower and upper surfaces of the plate respectively. The corresponding relation for the lift coefficient is

$$C_L = \int_0^c (p_l - p_u)\, dx / \tfrac{1}{2}\rho u_{ref}^2 c \tag{23}$$

where

$$p_l - p_u = -\mu\left[\int_0^x \left(\frac{\partial \zeta}{\partial y}\right)_l dx - \int_0^x \left(\frac{\partial \zeta}{\partial y}\right)_u dx\right]$$

The difficulty in achieving a solution with finite velocity at the neighborhood of the trailing edge of the plate has been partially solved by first placing both the leading and trailing edges within a finite element and not at a nodal point. The pressure at the trailing edge was then considered to be the average value of that on the rearmost nodal points on the lower and upper surfaces near the trailing edge. The pressure distribution on the upper and lower surfaces of the plate was then recalculated by solving the equation:

$$\left.\frac{\partial^2 p}{\partial x^2}\right|_{y=0} = \nu \left.\frac{\partial^3 u}{\partial x \partial y^2}\right|_{y=0}$$

with the boundary conditions

at $x = 0$ (leading edge), $p = p_1$

at $x = c$ (trailing edge), $p = p_2 = \frac{1}{2}(p_u + p_l)_{TE}$

The values of p_u and p_l were obtained using Equations (19) and (20). The trailing edge problem was further discussed by Plotkin and Flugge-Lotz [20], Stewartson [21], and Chang [22].

6. RESULTS AND DISCUSSION

In this work, a vortex model with the data given in Table 1 is used to simulate the free stream turbulence as outlined in Section 3. The variation of the velocity components u', v and the vorticity ζ with time at some of the boundary points are shown in Figures 4, 5, and 6 where u' is the fluctuating component of velocity in the x direction defined as $u' = (u - u_{ref})$. On the same figures the variations of the variables (u', v, and ζ), which are obtained from the finite element solution, at a point downstream of the plate are also plotted. The variation of the vorticity ζ at this point (see Figure 6) was considerably higher than that at any other boundary point and this is to be expected in the wake region of the plate. The variation of u' at the same point (see Figure 4) shows that it has a negative value over most of the sample time and this is expected because of the momentum deficit that occurred due to the drag force on the plate.

Table 1. Details of Vortex Model Parameters

Flow Statistics
Mean Flow Velocity, $u_{ref} = 4$ cm s^{-1}
Turbulence Intensity, $\frac{\langle u'^2 \rangle^{1/2}}{u_{ref}} = 0.357$
Length Scale, $L_{11}(x_1) = 9.85$ mm
Flatness Factor of u_1 Velocity Component = 3 (Gaussian distributed)
Vortex Model
Mean Convection Velocity (u_c) = 4 cm s^{-1}
Model Width (b) = 25 mm
Model Stage Length (s) = 20 mm
Number of Vortices per Box = 4
Vortex Core Radius (r_c) = 2.8 mm
Mean Distance Between Vortices (λ) = 11.2 mm
Vortex Circulation Constant (Γ_1) = 40 mm^2 s^{-1}

Figure 7 shows the variation of the drag coefficient of the upper and lower sides of the plate with time. Although the variation of drag coefficient on each individual side of the plate is considerable, the total drag coefficient is found to have small variation with time. A comparison between the total drag coefficient obtained from the present solution and the one obtained from Blasius solution, based on steady laminar flow with $u = u_{ref}$, showed that the two coefficients are very close over most of the sample time as can be seen in Figure 7. This should not be considered as a general conclusion for the case of a turbulent flow approaching a flat plate because flows with other statistical descriptions and higher Reynolds numbers were not studied in this work.

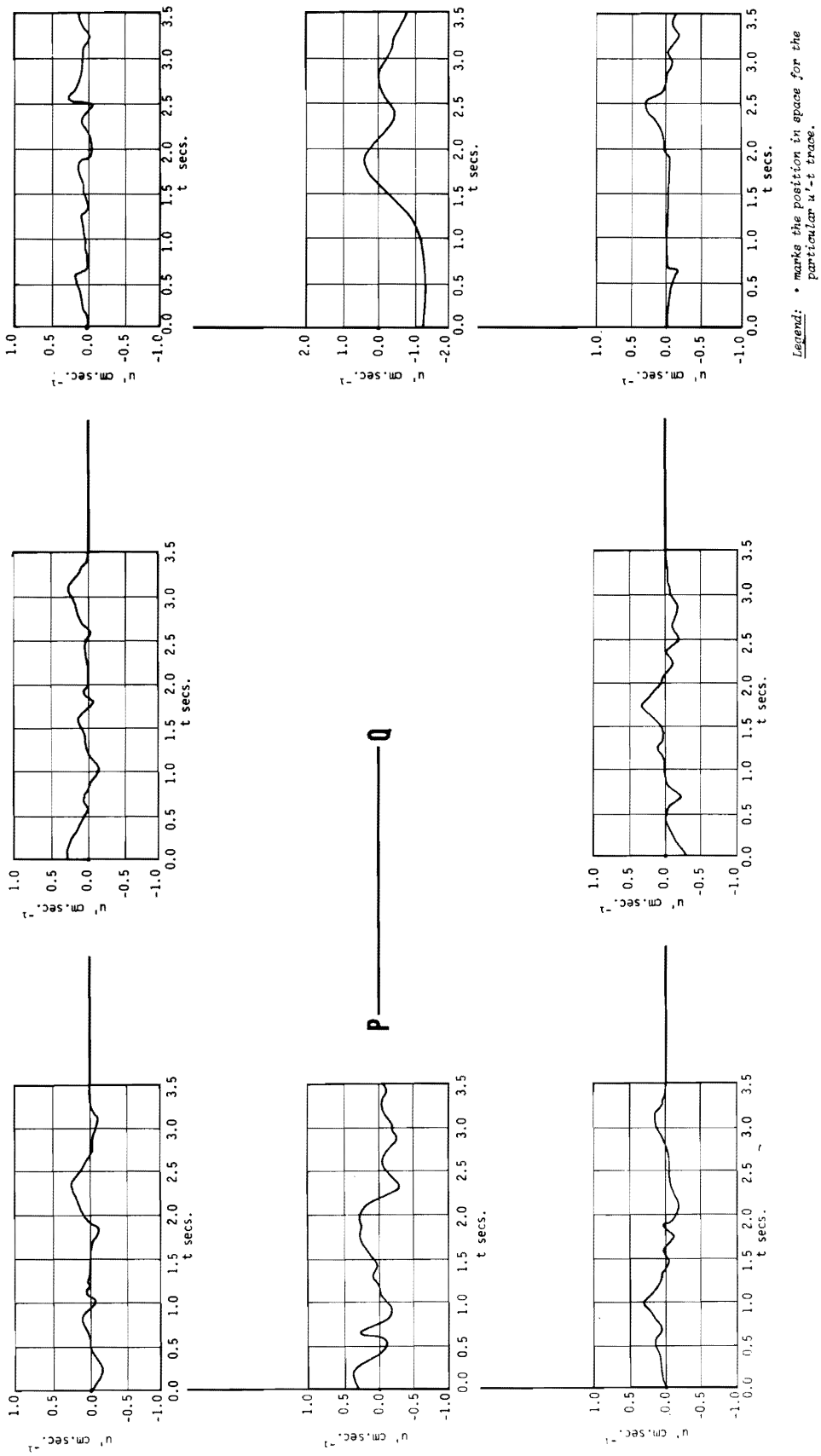

Figure 4. Variation of the Fluctuating Component of the Velocity u' with Time at Some Points in the Flow Field.

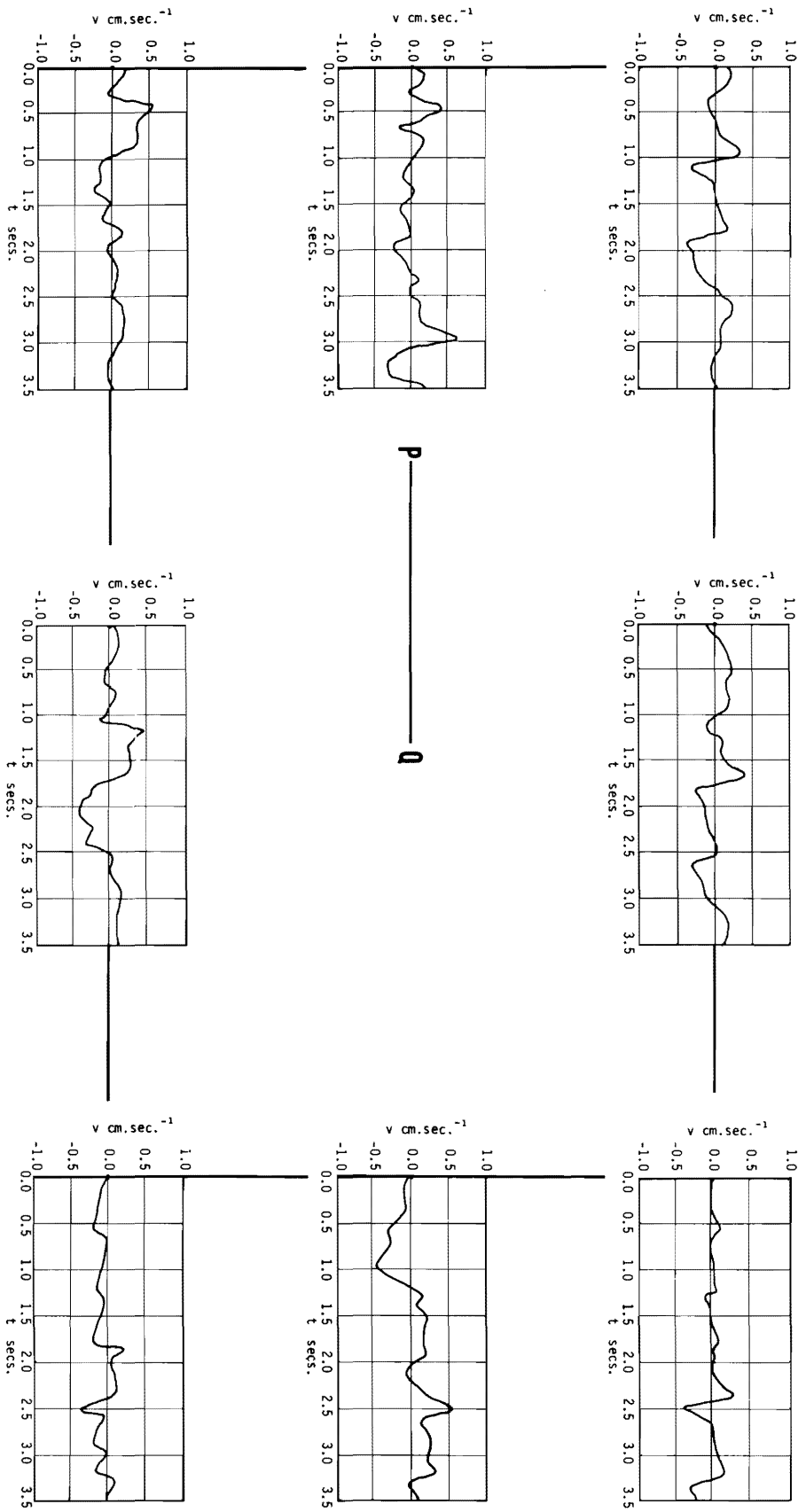

Figure 5. Variation of the v Component of the Velocity with Time at Some Points in the Flow Field.

Legend: • *marks the position in space for the particular v-t trace.*

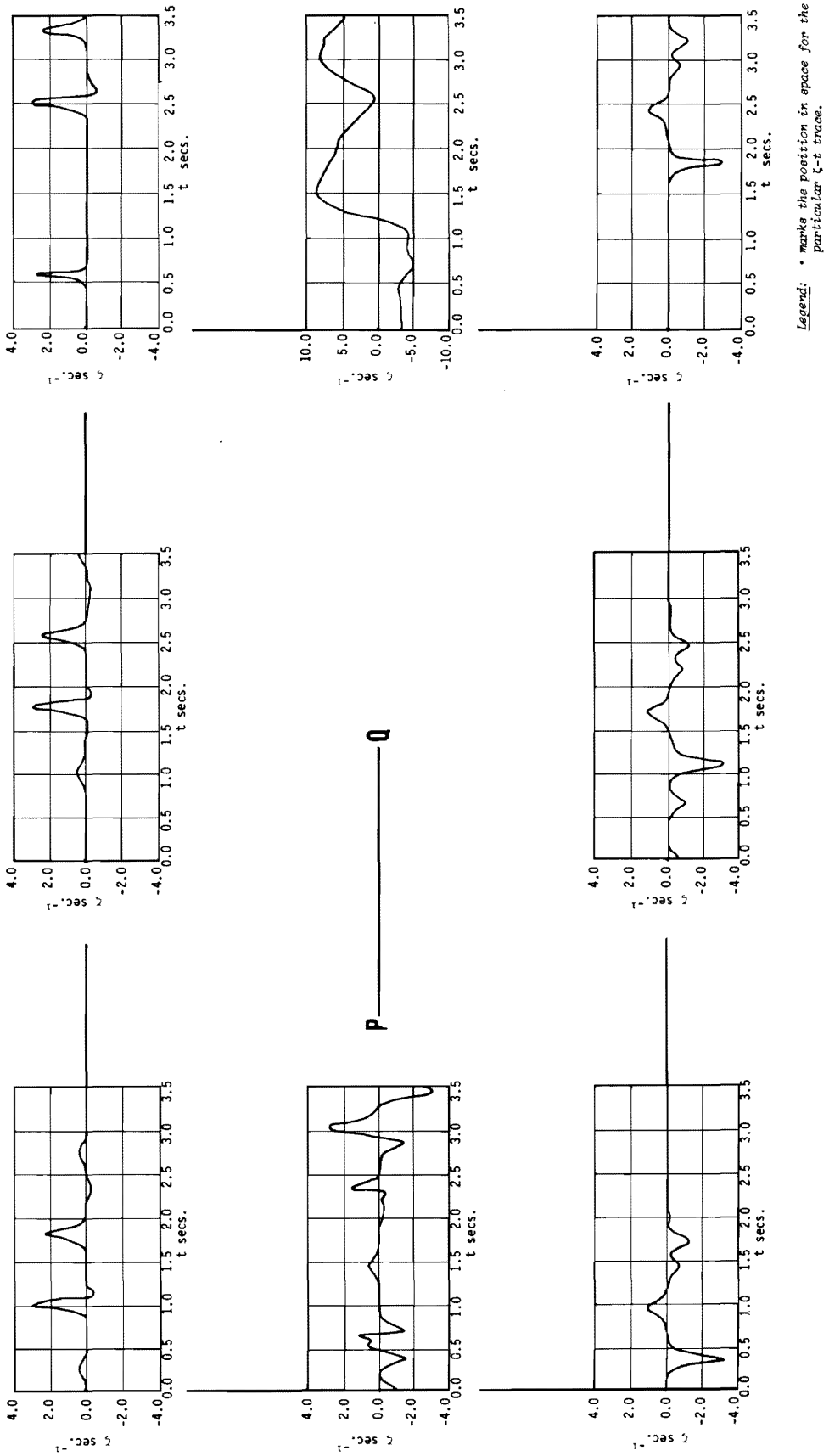

Figure 6. Variation of the Vorticity with Time at Some Points in the Flow Field.

The variation of lift coefficient C_L with time is shown in Figure 8 and illustrates how with this method of solution an actual time variation of the forces on the plate can be achieved. It may be noted that this increment in instantaneous lift force is due primarily to the imposed pressure field of the approaching

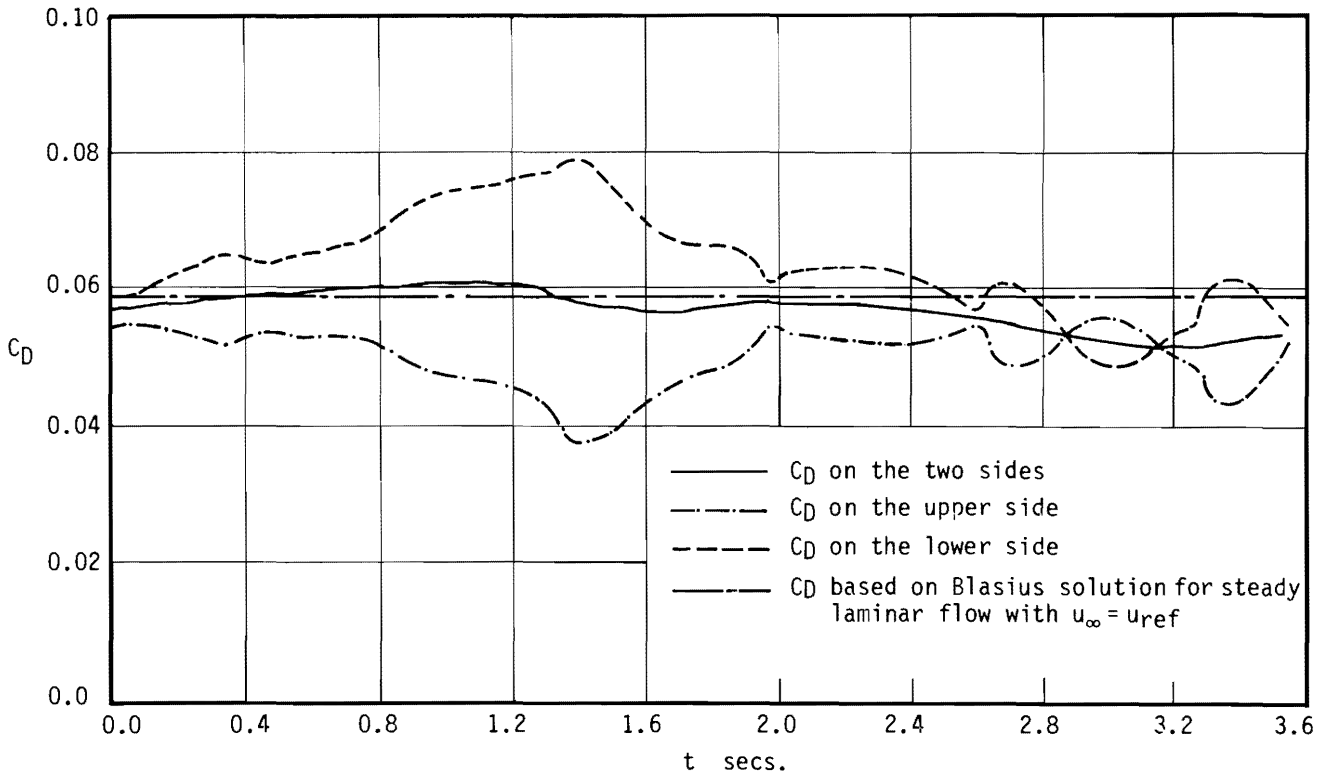

Figure 7. Variation of Plate Drag Coefficients with Time.

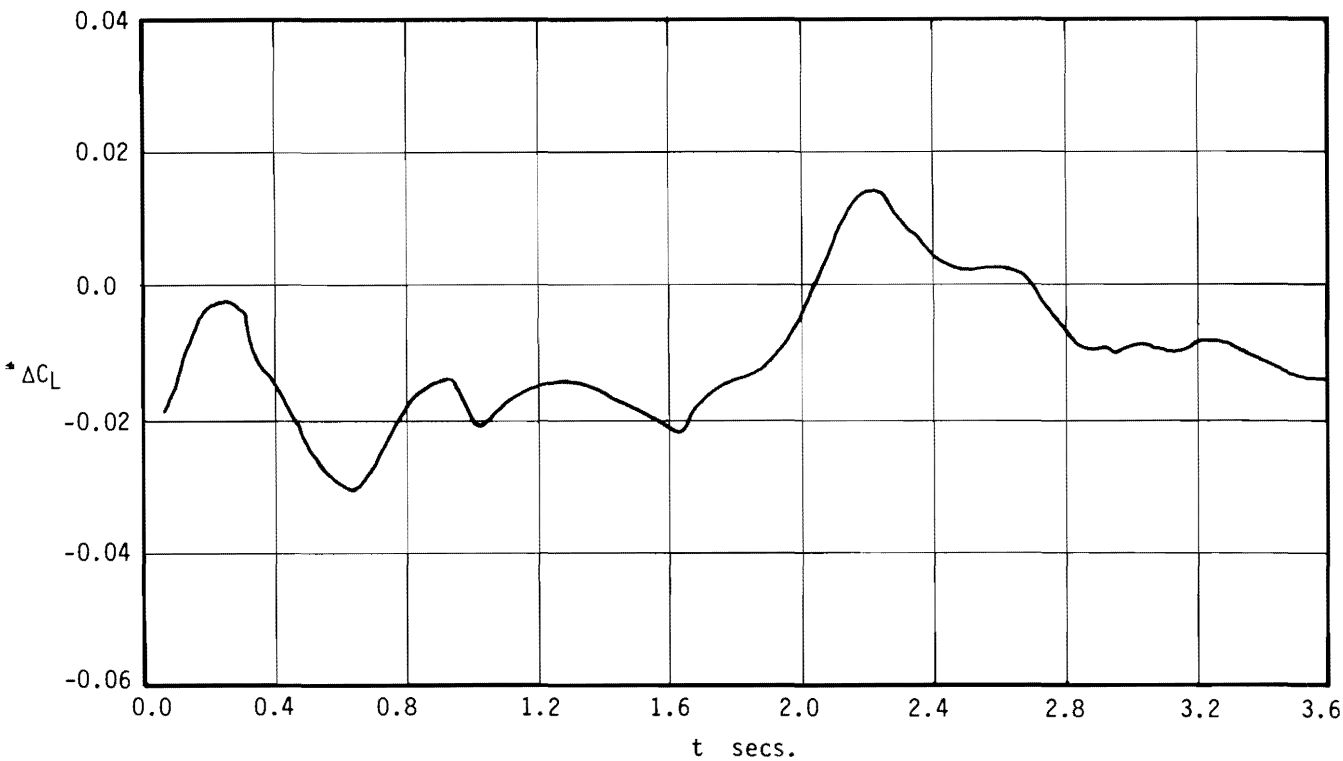

Figure 8. Variation of Lift Coefficient with Time.

rotational flow. However, for a long time span, the average lift coefficient for this flow regime would be zero.

7. CONCLUSIONS

The equations governing the unsteady, incompressible viscous flow over a thin flat plate were solved numerically using the variational approach. Equally important is the fact that the outer conditions of the finite element mesh set around the plate are unsteady, continuous, and stochastic. The finite element approach presented is found to be extremely stable and the effect of sudden change of the flow direction at a fixed point on the method of solution is simply an increase in the number of iterations to achieve convergence. The method predicted the response of the velocity and pressure fields in the vicinity of the plate to the disturbances in the free stream. The method also predicted the time variation of the lift and drag forces acting on the plate.

Other methods to predict the loads on flat surfaces and aerofoils due to free stream turbulence are based on the spectral approach. It is the opinion of the authors that a spectral analysis of turbulence when considering the loads on a flat plate or an aerofoil in a turbulent stream could be insufficient or perhaps even misleading.

REFERENCES

[1] D. K. Lilly, "Numerical Solution of Developing and Decaying Two-Dimensional Turbulence", *Journal of Fluid Mechanics,* **45** (1971), p. 395.

[2] G. Ahmadi and V. W. Goldschmidt, "Creation of a Pseudo-Turbulent Velocity Field", *Developments in Mechanics, vol. 6; Proceedings of the 12th Midwestern Conference,* (1972), p. 291.

[3] A. J. Chorin, "Numerical Study of Slightly Viscous Flow", *Journal of Fluid Mechanics,* **57** (1973), p. 785.

[4] U. Frisch, M. Lesieur, and A. Brissaud, "A Markovian Random Coupling Model for Turbulence", *Journal of Fluid Mechanics,* **65** (1974), p. 145.

[5] U. Schumann, G. Grotzbach, and L. Kleiser, *"Direct Numerical Simulation of Turbulence"*, ed. W. Kollmann. Hemisphere, 1980.

[6] C. Taylor, K. Morgan, and C. A. Brebbia, *Proceedings of the First International Conference on Numerical Methods in Laminar and Turbulent Flow, held at U. C. Swansea,* 1978. *Pentech Press.*

[7] W. C. Reynolds and R. W. Maccormack, *Proceedings of the Seventh International Conference on Numerical Methods in Fluid Dynamics.* Springer-Verlag, 1980.

[8] T. E. Base, "Mathematical Studies of Vortex Model to represent Unsteady Fluid Flow", *Ph. D. Thesis, I. S. V. R., The University of Southampton, England,* 1970.

[9] T. E. Base and P. O. Davies, "A Vortex Model to Relate Eulerian and Lagrangian Velocity Fields", *Canadian Journal of Chemical Engineering,* **52** (1974), p. 11.

[10] J. Van der Vooren and T. E. Labrujere, "Finite Element Solution of the Incompressible Flow over an Airfoil in a Non-uniform Field", *Proceedings of the International Conference for Numerical Methods in Fluid Dynamics held at the University of Southampton, England,* September 26-28, 1973.

[11] T. Bratanow, A. Ecer, and M. Koboske, "Numerical Calculations of Velocity and Pressure Distribution around Oscillating Aerofoils", *NASA CR – 2368,* 1974.

[12] T. Bratanow and A. Ecer, "On the Application of Finite Element Method in Unsteady Aerodynamics", *American Institute of Aeronautics and Astronautics Journal,* **12** (1974), p. 503.

[13] T. Bratanow and A. Ecer, "Analysis of Three-Dimensional Unsteady Viscous Flow around Oscillating Wings", *American Institute of Aeronautics and Astronautics Journal,* **12** (1974), p. 1577.

[14] R. T. Cheng, "Numerical Solution of the Navier–Stokes Equations by the Finite Element Method", *in The Physics of Fluids,* **15** (1972), p. 2098.

[15] C. Taylor and P. Hood, "A Numerical Solution of the Navier–Stokes Equations using the Finite Element Technique", *Computers and Fluids,* **1** (1973), p. 73.

[16] T. Kawai, "Finite Element Flow Analysis", *Proceedings of the Fourth International Symposium on Finite Element Methods in Flow Problems, Chuo University, Tokyo, 1982.* University of Tokyo Press and North-Holland.

[17] C. Taylor, J. A. Johnson, and W. R. Smith, "Numerical Methods in Laminar and Turbulent Flow", *Proceedings of the Third International Conference on Numerical Methods in Laminar and Turbulent Flow held in Seattle, USA.* Pineridge Press, 1983.

[18] H. M. Badr and T. E. Base, "A Variational Finite Element Method for Solving Unsteady Viscous Flow Problems", *Trans. CSME,* **5** (1978-79), p. 39.

[19] H. Schlichting, "Boundary Layer Theory". New York: McGraw-Hill, 1968.

[20] A. Plotkin and I. Flugge-Lotz, "Numerical Solution for the Laminar Wake Behind a Finite Flat Plate", *Journal of Applied Mechanics, Transaction ASME,* **45** (1968), p. 625.

[21] K. Stewartson, "On the Flow Near the Trailing Edge of a Flat Plate", *Mathematika,* **16** (1969), p. 106.

[22] G. Z. Chang, "Numerical Solutions for Viscous Fluid Flow in Two-Dimensions", *Ph. D. Thesis, The University of Western Ontario, London, Canada,* 1970.

Paper Received 28 October 1985; Revised 19 March 1986.